metals

MDPI

Article

Investigation on Blood Compatibility of Cu/Ti Metal Coating Prepared via Various Bias Voltages and Copper Content

Qiong Hu [1], Hengquan Liu [1,*], Fei Gao [2,*], Xi Yang [1], Junfeng Li [1], Ren Liu [3], Zexuan Liu [1] and Dongfang Wang [1]

[1] College of Materials and Chemistry & Chemical Engineering, Chengdu University of Technology, Chengdu 610059, China; qiongqhu@163.com (Q.H.); yangxi926494@163.com (X.Y.); lijunfeng@cdut.cn (J.L.); linzexuan@hotmai.com (Z.L.); wangdongfang2021@163.com (D.W.)
[2] Chengdu Neurotrans Medical Technology Co., Ltd., Chengdu 610094, China
[3] Department of Research & Development, Chengdu Medtech-Life Co., Ltd., Chengdu 610094, China; medtechlife@aliyun.com
* Correspondence: liuhengquan15@cdut.edu.cn (H.L.); phil.gao@neurotrans.com.cn (F.G.)

Abstract: Surface modification of some metal coatings is usually used to improve the blood compatibility of biomaterials; however, some aspects of the bological properties of metal coatings cannot be adjusted via the content of each component. In this work, Cu/Ti metal coatings with various amounts of copper content were prepared by the physical vapor deposition (PVD) method, and the influence of deposition bias was further investigated. Phase structure, element composition and surface morphology were investigated by X-ray diffraction (XRD), X-ray photoelectron spectroscopy (XPS) and scanning electron microscopy, respectively. The hemolysis ratio, platelet adhesion and protein adsorption were applied to evaluate the blood compatibility. The results show that a Cu/Ti coating of uniform quality can be obtained; the dispersion of the deposition and copper content is regulated by the number of copper sheets, but the deposition bias does not obviously affect the copper content of the Cu/Ti coating. The hemolysis rate of the Cu/Ti coating is less than 0.4%, the degree of platelet adhesion is significantly reduced on Cu/Ti coatings compared to control samples, and the contact angle of all coatings is greater than that of pure titanium. The largest adsorption capacity of BSA was found on the coating with the deposition bias voltage of −40 V. The number of copper flakes is increased, and the adsorption of FIB on the Cu/Ti coating surface is reduced. Therefore, Cu/Ti coatings prepared via this deposition method have potential for applications to regulate blood compatibility and surface performance.

Keywords: Cu/Ti coating; bias voltage; copper content; blood compatibility

Citation: Hu, Q.; Liu, H.; Gao, F.; Yang, X.; Li, J.; Liu, R.; Liu, Z.; Wang, D. Investigation on Blood Compatibility of Cu/Ti Metal Coating Prepared via Various Bias Voltages and Copper Content. *Metals* **2022**, *12*, 435. https://doi.org/10.3390/met12030435

Academic Editor: Sergey N. Grigoriev

Received: 21 January 2022
Accepted: 20 February 2022
Published: 1 March 2022

1. Introduction

Cardiovascular disease (CVD) is one of the major causes of human mortality around the world. The latest report shows that the death count caused by CVD is approximately half of all deaths [1]. The current, most effective treatment method of CVD is interventional therapy with a vessel stent. After the stent is implanted in the body, the surface of the stent material will interact with the physiological components; protein adsorption and activation, blood cell destruction and an intimal increase occur at the interface between the material and blood. In order to improve the blood compatibility of the stent surface, some researchers have reported that surface modification of inorganic coatings of the stent surface can be employed to improve blood compatibility, such as a Ti-O coating [2–4], TiN coating [5,6], diamond-like carbon [7–12], etc. Although the blood compatibility has been improved via these inorganic coatings, the above coatings cannot be widely used in vascular stents because of their brittleness.

Titanium alloys have been widely used as biological materials on account of their low density, non-magnetic nature [13], light weight [14], good corrosion resistance [15], high fatigue strength [16] and good biocompatibility [17,18]. Copper is an essential element for

the normal growth of organisms and the development of tissue structure [19–21], and it plays an important role in the homeostasis, inflammation, proliferation and remodeling of wound healing. H Liu et al. [22,23] successfully prepared Cu/Ti coatings by vacuum arc source deposition and physical vapor deposition. The study found that Cu/Ti coatings were less toxic to endothelial cells and showed good biocompatibility. At the same time, Cu/Ti coatings present a good inhibitory effect, but the Cu/Ti coatings prepared by vacuum arc plasma deposition easily contain micro-sputtered particles, which affect the continuity of the damaged coatings. D Wojcieszak et al. [24] reported that Cu/Ti coatings were prepared by magnetron co-sputtering (Ti target and Cu target); the result showed that Cu/Ti coatings were less toxic towards fibroblasts. While their work focused on the bactericidal activity and cytotoxicity of the Cu/Ti coating, its blood compatibility was not mentioned, and there are higher requirements for the magnetron sputtering equipment.

In order to obtain a uniform and smooth Cu/Ti metal coating, the magnetron sputtering of a single target was employed to prepare it, and the copper content and morphology of the Cu/Ti composite coating were regulated by changing the number of copper sheets and the bias voltage. The blood compatibility of Cu/Ti coatings with different deposition bias and copper content was also investigated.

2. Materials and Methods

2.1. Preparation of Cu/Ti Metal Coatings

Single target sputtering by magnetron sputtering was adopted to prepare Cu/Ti composite coatings. A certain number and size of copper sheets were placed on the titanium target. The copper–titanium composite target with different copper–titanium content could be prepared by adjusting the quantity and size of copper sheets. Cu/Ti composite coatings with different copper content were prepared under a certain sputtering process.

The Cu/Ti metal coating was prepared on a medical titanium surface (10 mm × 10 mm) by magnetron sputtering. A titanium target with a diameter of 50.0 mm and a purity of 99.99% and a copper sheet with a diameter of 10 mm and a purity of 99.999% were used in the preparation process. Prior to the deposition of the coating, the surface of the medical titanium substrate was polished with different waterproof sandpapers; then, the substrate was ultrasonically cleaned in acetone and anhydrous ethanol for 10 min, and the treated medical titanium was placed in a vacuum chamber. At the beginning of coating preparation, the pressure in the vacuum chamber was pumped to 6×10^{-4} Pa by a mechanical pump and molecular pump, and the flow rate of argon gas was 120 SCCM. When the pressure of the vacuum chamber reached 2.0 Pa, a bias of −700 V was applied, and the surface of the sample was bombarded with argon ions for 10 min. Regarding the deposition process, the technical parameters of sputtering and detailed data are shown in Table 1.

Table 1. The preparation parameters of various Cu/Ti coatings.

Sample No	Sputtering Pressure (Pa)	Sputtering Power (W)	Sputtering Bias (V)	Deposition Time (min)	Copper Number (Slice)
1#	0.4	100	0	60	1
2#	0.4	100	−40	60	1
3#	0.4	100	−80	60	1
4#	0.4	100	−120	60	1
5#	0.4	100	−40	60	2
6#	0.4	100	−40	60	3

2.2. Coating Characterization

The surface morphology and phase structure of the coatings was characterized by field emission scanning electron microscopy (SEM, FEI INSPECT F50, Hillsboro, OR, USA) and X-ray diffraction (XRD, D2 PHASER, Bruker, Billerica, MA, USA). X-ray photoelectron spectroscopy (XPS, VG Science, East Grinstead, UK) was used to detect the chemical

composition and chemical valence state of the coating surface and the interior. To study the wettability of the coating surface, a liquid–solid wetting angle analyzer (SDC-200, SINDIN, Dongguan, China) was used to examine the hydrophilicity and hydrophobicity of the coating.

2.3. Blood Compatibility

2.3.1. Hemolysis Ratio

The hemolysis assay was performed in accordance with ISO 109934:2009 (National standard for hemolysis rate). We added 8 mL of anticoagulant blood to a container containing 10 mL 0.9% sodium chloride injection, and gently shook the mixture to prepare diluted blood; the absorbance at 545 nm was obtained with an ultraviolet spectrophotometer. The hemolysis ratio was calculated according to the following formula:

$$HR\ (\%) = (A - A_1)/(A_2 - A_1) \times 100\% \quad (1)$$

where HR is the hemolysis ratio (%), A is the absorbance of the sample (%), A_1 is the absorbance of the negative controls (%) and A_2 is the absorbance of the positive control (%).

2.3.2. Platelet Adhesion

We centrifuged the fresh human blood and removed the supernatant. The coated sample was ultrasonically cleaned with absolute ethanol and distilled water. The sample was soaked in platelet-rich plasma (PRP), and then incubated in a constant-temperature water bath at 37 °C for 2 h. After rinsing the samples with phosphate-buffered saline (PBS), the samples were fixed with 2% glutaraldehyde for 4 h, and then dehydrated with ethanol at concentrations of 50%, 70%, 90% and 100%. After drying, the platelet adhesion number and morphology were observed under the scanning electron microscope.

2.3.3. Platelet Activation

PRP was obtained by centrifugation of fresh whole blood containing sodium citrate. We spread the platelet-rich plasma fully on the surface of the sample (10 mm × 10 mm), incubated it at 37 °C for 2 h and washed it with bovine serum albumin solution 3 times. Subsequently, mouse anti-human CD62P antibody (primary antibody) was added, the sample was incubated at 37 °C for 1 h, and then a secondary antibody solution was added (goat anti-mouse polyclonal antibody labeled with horseradish peroxidase) and incubated at 37 °C for 1 h. Finally, we added the chromogenic agent and the material for 5–10 min, transferred the chromogenic solution to the microtiter plate, added sulfuric acid solution to stop the color, placed the sample in the microplate reader and calculated the platelet activation amount according to the optical density (OD) value.

2.4. Protein Adsorption

The Protein Quantification Kit (BCA Assay) was used to measure the adsorption behavior of the two main proteins (albumin, fibrinogen and globulin) in the plasma on the surface of the material. First, we prepared 1 mg/mL protein solution with PBS solution, equilibrated the coating surface (10 mm × 10 mm) with PBS solution for 2 h and then immersed it in 3 mL protein (albumin, fibrinogen, globulin) solution and allowed it to adsorb at 37 °C for 2 h. The coating was immersed in 2% sodium dodecyl sulfonate (SDS) solution and stirred at 37 °C for 2 h to fully resolve the surface-absorbed proteins into the SDS solution. The number of absorbed proteins was determined by using the corresponding kit for reaction and coloration.

3. Results and Discussion

3.1. Structure and Surface Topography of Thin Films

The XRD patterns of various Cu/Ti composite coatings are shown in Figure 1. The position of the titanium peak (100) of samples 2# and 3# is shifted from Figure 1a, and the

diffraction peaks of Ti are broadened more obviously. The broadening of the diffraction peaks may be because Cu is solid dissolved in Ti crystals to form a solid solution of Ti, causing lattice distortion, peak broadening and peak shifting.

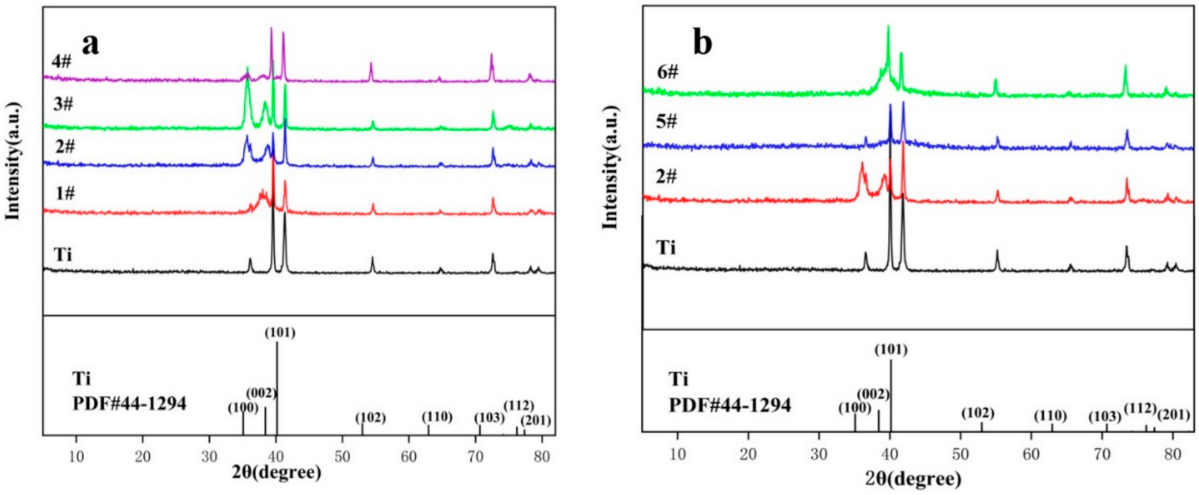

Figure 1. XRD pattern of Cu/Ti coating: (**a**) different bias voltage, (**b**) different number of copper sheets.

The number of copper sheets increases, the (100) peak is gradually reduced (Figure 1b), and the center of the XRD broadening peak gradually shifts to the right, which may be due to the formation of some Cu/Ti phases containing Cu at the same time [25], and it gradually increases with the increase in the copper content in the film.

Figure 2 shows the high-resolution spectra of Ti2p of samples 2# and 4#. The peaks of Ti2p1/2 and Ti2p3/2 appear at 464.1 eV and 458.6 eV, respectively, and the difference in the electron binding energy between the two is 5.7 eV, which indicates that the Ti on the film surface is oxidized into TiO_2 in the air. The Cu2p peak binding energies of elemental Cu and CuO only differ by 0.1 eV [26]. It is difficult to distinguish elemental Cu from Cu_2O by the Cu2p peak. However, it is reported in the literature that Cu on the surface of a film is easily oxidized, and Cu should exist in two forms, CuO and Cu_2O, and not contain elemental Cu [24].

Table 2 shows the element content of 1#, 2#, 3# and 4# samples. We found that with the increase in deposition bias, the content of copper and titanium did not change significantly.

Table 2. The element content of 1#, 2#, 3# and 4# samples.

Sample	Element Component (at%)		
	Ti	Cu	O
1#	20.04	0.49	79.47
2#	21.34	0.52	78.14
3#	22.91	0.54	76.55
4#	23.77	0.53	75.77

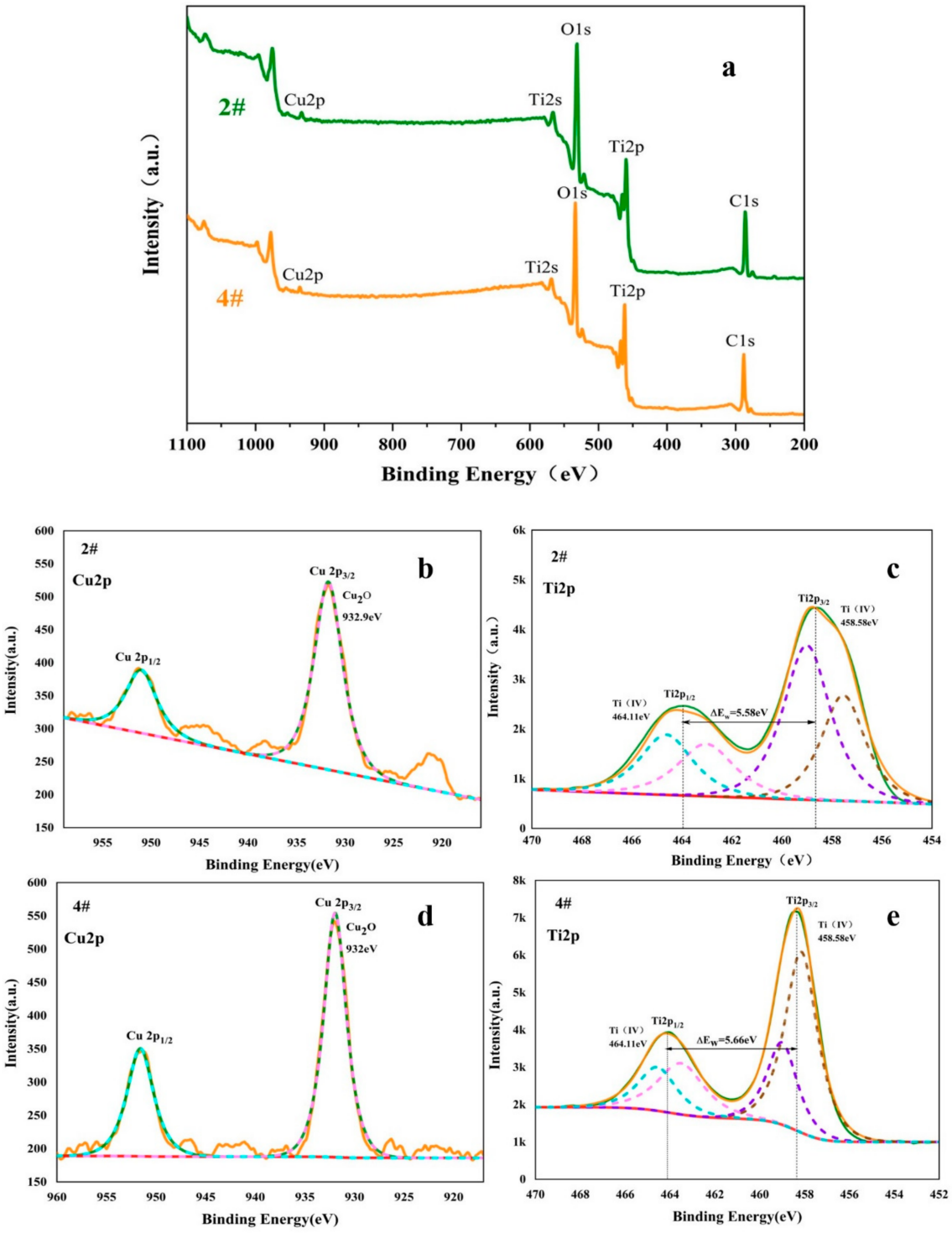

Figure 2. XPS spectra of 2# and 4# samples: (**a**) full spectrum, (**b**) 2# Cu2p, (**c**) 2# Ti2p, (**d**) 4# Cu2p, (**e**) 4# tip.

The SEM morphology of the Cu/Ti composite coatings is shown in Figure 3. It can be clearly observed that the surface of the Cu/Ti composite coating is uniform, and grain boundaries and obvious cracks are not found. All coatings show directional streaks, which may be caused by grinding of the substrate. The surface smoothness of the Cu/Ti coating first increases and then decreases following the increase in the bias voltage. A suitable energy is conducive to the migration of sputtered atoms under a suitable deposition bias;

thereby, the surface smoothness would be increased. Some particles were observed on the surface of the 4# coating and distinct crystal boundaries between the particles were also found. These results might be due to the introduction of bias, leading to the enhancement of the energy deposition effect, which was conducive to the growth of surface grains. It can be seen from Figure 3e–g that the density of sample 2# is higher than that of samples 5# and 6#: this is because the sputtering energy of copper is relatively low, so the Cu content of sample 6# is higher than that of sample 2# and sample 5#.

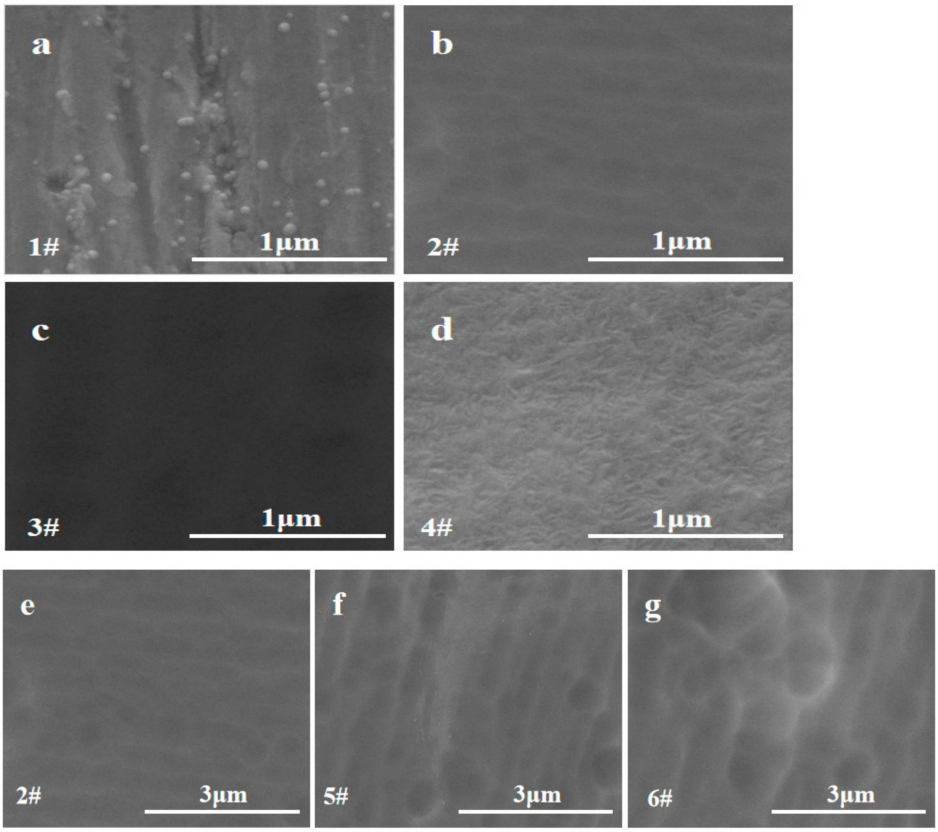

Figure 3. The SEM images of various Cu/Ti composite coatings: (**a**) 1#, (**b**) 2#, (**c**) 3#, (**d**) 4#, (**e**) 2#, (**f**) 5#, (**g**) 6#.

3.2. Surface Wetting Test

The biological behaviors of cell adhesion, proliferation and migration on the material surface are affected by the wettability of the material surface [26,27]. The surface wettability angle and surface energy of various coatings are shown in Figure 4a,b, respectively. The contact angle of medical titanium is the smallest, which is approximately 67°. The contact angle of the Cu/Ti composite coating is larger than that of medical titanium.

The free energy of the Cu/Ti composite coating is less than that of medical titanium, as shown in Figure 4c,d. The higher the surface free energy of the coating, the smaller the contact angle and the better the water droplet wettability.

The hemolysis rates of all Cu/Ti coatings was less than 0.4, which is in accordance with the ISO 10993-4:2002 standard; it indicates that all Cu/Ti composite coatings were safe.

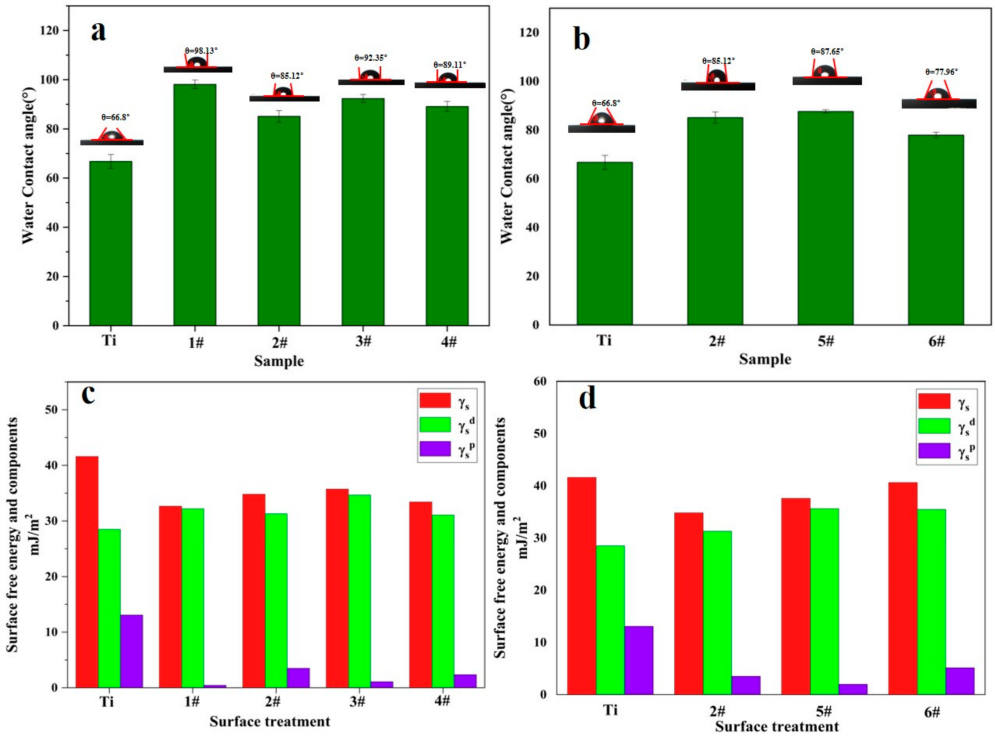

Figure 4. The contact angle and surface energy of various samples: (**a**) the contact angle of 1#–4#, (**b**) the contact angle of 2#, 5# and 6#, (**c**) free energy of 1#–4#, (**d**) free energy of 2#, 5# and 6#.

3.3. Platelet Adhesion and Activation

Platelet adhesion and activation are the main causes of thrombosis. The platelet adhesion on the surface of medical titanium is shown in Figure 5a. Platelets spread across a large area were found, and the platelet aggregation and activation were very evident. Figure 5b–e show that, compared to medical titanium, the adhesion and aggregation of platelets on the Cu/Ti coating surface prepared under a certain deposition bias were reduced. It can be seen from Figure 5g,h that the number of platelets adsorbed by the samples is significantly reduced, and the shape is almost round, without aggregation and spreading behavior.

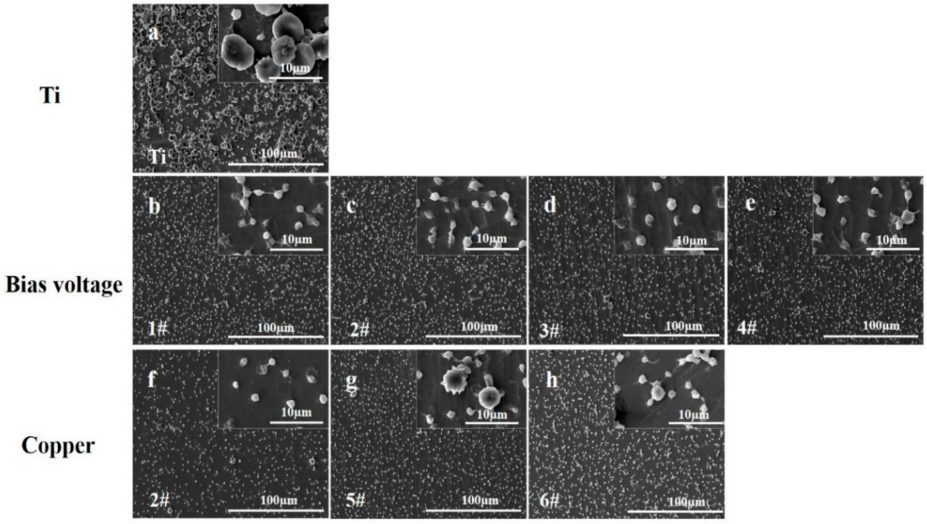

Figure 5. Platelet adhesion of Cu/Ti composite coatings: (**a**) Ti, (**b**) 1#, (**c**) 2#, (**d**) 3#, (**e**) 4#, (**f**) 2#, (**g**) 5#, (**h**) 6#.

The activation of platelets of various samples is described in Figure 6. These samples were different from the Cu/Ti coatings prepared with various parameters such as bias voltage and number of copper sheets. It can be seen from Figure 6a that the deposition bias is increased, and the effect of inhibiting platelet activation becomes greater, which may be related to the density and smoothness of the coating surface. Figure 6b shows the platelet activation under different numbers of copper plates. The platelet activation on the surfaces of samples 2#, 5# and 6# is inhibited. As the number of copper plates increases, the amount of platelet activation shows an increasing trend.

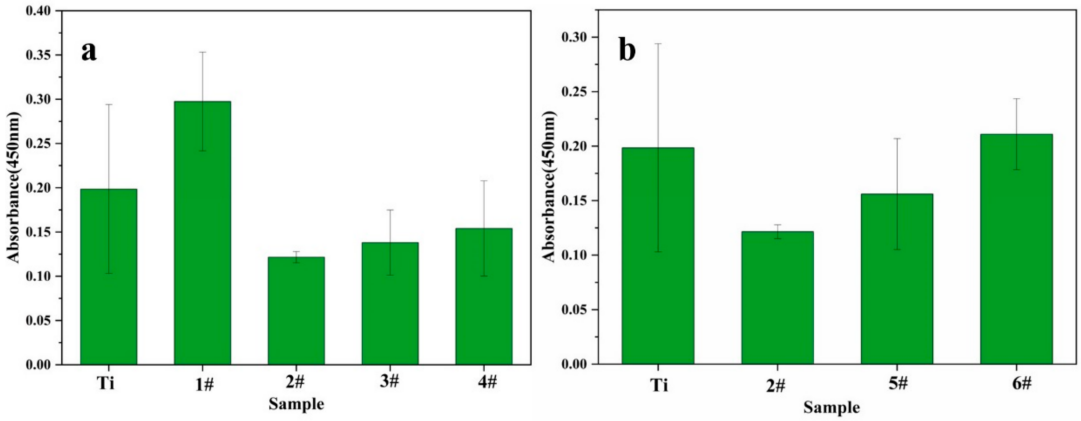

Figure 6. The platelet activation. (**a**) Different bias voltage, (**b**) different copper content.

3.4. Protein Adsorption

The Protein Quantification Kit (BCA Assay) method was used to further study the adsorption of proteins. The adsorption of albumin can reduce the adhesion and activation of platelets; thereby, the coagulation performance of the material's surface would be inhibited [28]. On the contrary, the blood compatibility of the material would be reduced owing to the adsorption and denaturation of fibrinogen (FIB) [29]. The adsorption of Bulked Segregant Analysis (BSA) and FIB on the Cu/Ti composite coating is shown in Figure 7. It can be seen from Figure 7a that the amount of BSA adsorbed on the surface of sample 4# is the largest, and the amount of FIB adsorbed on the surface of sample 2# is the largest. It can be found that the adsorption amount of BSA on the surfaces of samples 2#, 5# and 6# increases with the increase in copper content, as shown in Figure 7b.

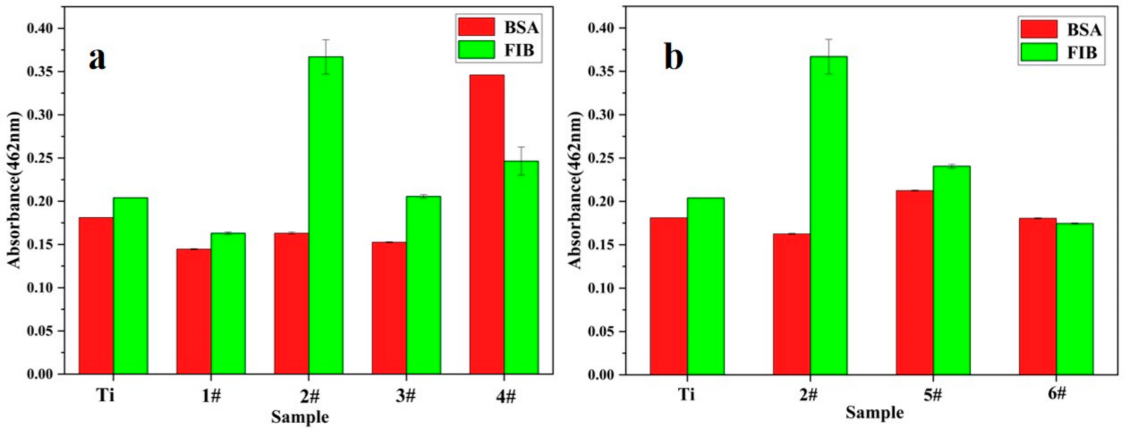

Figure 7. Surface fibrinogen and albumin adsorption capacity on various surfaces (indicated by OD value). (**a**) Different bias voltage, (**b**) different copper content.

4. Conclusions

In this study, a Cu/Ti composite coating was successfully prepared by magnetron single-target sputtering, and its surface wettability, protein adsorption and blood compatibility were affected by the deposition bias and copper content. The main conclusions are as follows.

(1) The copper content of various coatings is mainly determined by the number of copper sheets; the deposition bias was detected as a due to the influence of the quality of the coating.
(2) As the deposition bias increases, the smoothness and density of the coating are first increased and then decreased.
(3) The maximum amount of BSA adsorption occurs when the deposition bias voltage is −40 V. With the increase in the number of copper sheets, the adsorption amount of FIB gradually decreases.
(4) The Cu/Ti coatings prepared with different bias voltages and different numbers of copper sheets significantly reduced platelet adhesion, and the degree of platelet activation on the coating surface gradually increased.
(5) The results demonstrate that Cu/Ti composite coatings could improve the blood compatibility; this research result can be used for the surface modification of blood contact materials.

Author Contributions: Conceptualization, H.L. and F.G.; methodology, Q.H.; software, Q.H.; validation, X.Y., D.W. and Z.L.; formal analysis, Q.H.; investigation, J.L.; resources, H.L., R.L. and F.G.; data curation, Q.H.; writing—original draft preparation, Q.H.; writing—review and editing, H.L. and Q.H.; visualization, H.L.; supervision, H.L. and J.L.; project administration, H.L.; funding acquisition, H.L. All authors have read and agreed to the published version of the manuscript.

Funding: This work was jointly and financially supported by the Sichuan Science and Technology Program (Grant No. 2020JDRC0070). This study was also supported by the Jiangsu Province Engineering Research Center for Biomedical Materials and Advanced Medical Devices.

Data Availability Statement: Not applicated.

Conflicts of Interest: The authors declare no conflict of interest.

References

1. Arora, S.; Stouffer, G.A.; Kucharska-Newton, A.M.; Qamar, A.; Vaduganathan, M.; Pandey, A.; Porterfield, D.; Blankstein, R.; Rosamond, W.D.; Bhatt, D.L.; et al. Twentyyear trends and sex differences in young adults hospitalized with acute myocardial infarction. *Circulation* **2019**, *139*, 1047–1056. [CrossRef] [PubMed]
2. Zong, M.; Bai, L.; Liu, Y.; Wang, X.; Zhang, X.; Huang, X.; Hang, R.; Tang, B. Antibacterial ability and angiogenic activity of Cu–Ti–O nanotube arrays. *Mater. Sci. Eng. C* **2017**, *71*, 93–99. [CrossRef] [PubMed]
3. Liu, Y.; Hang, R.; Zhao, Y.; Bai, L.; Sun, Y.; Yao, X.; Jia, H.; Tang, B.; Hang, R. The effects of annealing temperature on corrosion behavior, Ni2+ release, cytocompatibility, and antibacterial ability of Ni–Ti–O nanopores on NiTi alloy. *Surf. Coat. Technol.* **2018**, *352*, 175–181. [CrossRef]
4. Hang, R.; Liu, Y.; Bai, L.; Zong, M.; Wang, X.; Zhang, X.; Huang, X.; Tang, B. Electrochemical synthesis, corrosion behavior and cytocompatibility of Ni–Ti–O nanopores on NiTi alloy. *Mater. Lett.* **2017**, *202*, 5–8. [CrossRef]
5. Lin, N.; Huang, X.; Zou, J.; Zhang, X.; Qin, L.; Fan, A.; Tang, B. Effects of plasma nitriding and multiple arc ion plating TiN coating on bacterial adhesion of commercial pure titanium via in vitro investigations. *Surf. Coat. Technol.* **2012**, *209*, 212–215. [CrossRef]
6. Hussein, M.A.; Ankah, N.K.; Kumar, A.M.; Azeem, M.A.; Saravanan, S.; Sorour, A.A.; Al Aqeeli, N. Mechanical, biocorrosion, and antibacterial properties of nanocrystalline TiN coating for orthopedicapplications. *J. Ceram. Int.* **2020**, *46*, 18573–18583. [CrossRef]
7. Liao, T.T.; Zhang, T.F.; Li, S.S.; Deng, Q.Y.; Wu, B.J.; Zhang, Y.Z.; Zhou, Y.J.; Guo, Y.B.; Leng, Y.X.; Huang, N. Biological responses of diamond-like carbon (DLC) films with different structures in biomedical application. *J. Mater. Sci. Eng. C* **2016**, *69*, 751–759. [CrossRef]
8. Choudhury, D.; Ching, H.A.; Mamat, A.B.; Cizek, J.; Abu Osman, N.A.; Vrbka, M.; Hartl, M.; Krupka, I. Fabrication and characterization of DLC coated microdimples on hip prosthesis heads. *J. Biomed. Mater. Res. Part B* **2015**, *103*, 1002–1012. [CrossRef]
9. Zhang, T.F.; Deng, Q.Y.; Liu, B.; Wu, B.J.; Jing, F.J.; Leng, Y.X.; Huang, N. Wear and Corrosion Properties of diamond like carbon (DLC) Coating on stainless steel, CoCrMo and Ti6Al4V substrate. *Surf. Coat. Technol.* **2015**, *273*, 12–19. [CrossRef]

10. Dhandapani, V.S.; Subbiah, R.; Thangavel, E.; Arumugam, M.; Park, K.; Gasem, Z.M.; Veeraragavan, V.; Kim, D.-E. Tribological properties, corrosion resistance and biocompatibility of magnetron sputtered titanium-amorphous carbon coatings. *Appl. Surf. Sci.* **2016**, *371*, 262–274. [CrossRef]
11. Bociaga, D.; Sobczyk-Guzenda, A.; Szymanski, W.; Jedrzejczak, A.; Jastrzebska, A.; Olejnik, A.; Swiatek, L.; Jastrzebski, K. Diamond like carbon coatings doped by Si fabricated by a multi-target DC-RF magnetron sputtering method—Mechanical properties, chemical analysis and biological evaluation. *Vacuum* **2017**, *143*, 395–406. [CrossRef]
12. Peng, F.; Lin, Y.; Zhang, D.; Ruan, Q.; Tang, K.; Li, M.; Liu, X.; Chu, P.K.; Zhang, Y. Corrosion Behavior and Biocompatibility of Diamond-like Carbon-Coated Zinc: An In Vitro Study. *J. ACS Omega* **2021**, *6*, 9843–9851. [CrossRef] [PubMed]
13. Sha, X.; Xiao, N.; Guan, Y.; Yi, X. A first-principles investigation on mechanical and metallic properties of titanium carbides under pressure. *Mater. Sci. Technol.* **2018**, *34*, 1953–1958. [CrossRef]
14. Xiangyu, Z.; Meng, L.; Xiaojing, H.; Ruiqiang, H.; Xiaobo, H.; Yueyue, W.; Xiaohong, Y.; Bin, T. Antibacterial activity of single crystalline silver-doped anatase TiO_2 nanowire arrays. *J. Appl. Surf. Sci.* **2016**, *372*, 139–144.
15. Trino, L.D.; Dias, L.F.; Albano, L.G.; Bronze-Uhle, E.S.; Rangel, E.C.; Graeff, C.F.; Lisboa-Filho, P.N. Zinc Oxide Surface Functionalization and Related Effects on Corrosion Resistanceof Titanium Implants. *Ceram. Int.* **2018**, *44*, 4000–4008. [CrossRef]
16. Wang, R.; He, X.; Gao, Y.; Zhang, X.; Yao, X.; Tang, B. Antimicrobial property, cytocompatibility and corrosion resistance of Zn-doped ZrO_2/TiO_2 coatings on Ti6Al4V implants. *J. Mater. Sci. Eng. C* **2017**, *75*, 7–15. [CrossRef]
17. Chiang, H.-J.; Chou, H.-H.; Ou, K.-L.; Sugiatno, E.; Ruslin, M.; Waris, R.A.; Huang, C.-F.; Liu, C.-M.; Peng, P.-W. Evaluation of Surface Characteristics and Hemocompatibility on the Oxygen Plasma-Modified Biomedical Titanium. *Metals* **2018**, *8*, 513. [CrossRef]
18. Hu, H.; Zhang, W.; Qiao, Y.Q.; Jiang, X.Y.; Liu, X.; Ding, C. Antibacterial activity and increased bone marrow stem cell functions of Zn-incorporated TiO_2 coatings on titanium. *Acta Biomater.* **2012**, *8*, 904–915. [CrossRef]
19. Li, Y.; Liu, L.; Wan, P.; Zhai, Z.; Mao, Z.; Ouyang, Z.; Yu, D.; Sun, Q.; Tan, L.; Ren, L.; et al. Biodegradable Mg-Cu alloy implants with antibacterial activity for the treatment of osteomyelitis: In vitro and in vivo evaluations. *Biomaterials* **2016**, *106*, 250–263. [CrossRef]
20. Pohanka, M. Copper and copper nanoparticles toxicity and their impact on basic functions in the body. *Bratisl. Med. J.* **2019**, *120*, 397–409. [CrossRef]
21. Kornblatt, A.P.; Nicoletti, V.G.; Travaglia, A. The neglected role of copper ions in wound healing. *J. Inorg. Biochem.* **2016**, *161*, 1–8. [CrossRef] [PubMed]
22. Liu, H.; Zhang, D.; Shen, F.; Zhang, G.; Song, S. Hemocompatibility and anti-endothelialization of copper-titanium coating for vena cava filters. *J. Surf. Coat. Technol.* **2012**, *206*, 3501–3507. [CrossRef]
23. Liu, H.; Zhang, D.; Shen, F.; Zhang, G.; Song, S. Corrosion and ion release behavior of Cu/Ti film prepared via physical vapor deposition in vitro as potential biomaterials for cardiovascular devices. *J. Appl. Surf. Sci.* **2012**, *258*, 7286–7291. [CrossRef]
24. Wojcieszak, D.; Kaczmarek, D.; Antosiak, A.; Mazur, M.; Rybak, Z.; Rusak, A.; Osekowska, M.; Poniedzialek, A.; Gamian, A.; Szponar, B. Influence of Cu-Ti thin film surface properties on antimicrobial activity and viability of living cells. *J. Mater. Sci. Eng. C* **2015**, *56*, 48–56. [CrossRef]
25. Stranak, V.; Wulff, H.; Rebl, H.; Zietz, C.; Arndt, K.; Bogdanowicz, R.; Nebe, B.; Bader, R.; Podbielski, A.; Hubicka, Z.; et al. Deposition of thin titanium- copper films with antimicrobial effect by advanced magnetron sputtering methods. *Mater. Sci. Eng. C* **2011**, *31*, 1512–1519. [CrossRef]
26. Ghodselahi, T.; Vesaghi, M.A.; Shafiekhani, A.; Baghizadeh, A.; Lameii, M. XPS study of the Cu@Cu_2O core-shellnanoparticles. *J. Appl. Surf. Sci.* **2008**, *255*, 2730–2734. [CrossRef]
27. Wu, Y.; Simonovsky, F.I.; Ratner, B.D.; Horbett, T.A. The role of adsorbed fibrinogen in platelet adhesion to polyurethane surfaces: A comparison of surface hydrophobicity, protein adsorption, monoclonal antibody binding, and platelet adhesion. *J. Biomed. Mater. Res. A* **2005**, *74*, 722–738. [CrossRef]
28. Kim, C.H.; Khil, M.S.; Kim, H.Y.; Lee, H.U.; Jahng, K.Y. An improved hydrophilicity via electrospinning for enhanced cell attachment and proliferation. *J. Biomed. Mater. B* **2006**, *78*, 283–290. [CrossRef]
29. Liu, H.Q.; Siedlecki, C.A. (Eds.) *Hemocompatibility of Biomaterials for Clinical Applications*; Woodhead Publishing: Thorston, UK, 2018; pp. 379–394.